

# Differential measurements of jet sub-structure observables and their correlation in $p+p$ collisions at $\sqrt{s} = 200$ GeV in STAR

Monika Robotková for the STAR Collaboration\*

Nuclear Physics Institute of the CAS

\* robotmon@fjfi.cvut.cz

July 30, 2021



*Proceedings for the XXVIII International Workshop  
on Deep-Inelastic Scattering and Related Subjects,  
Stony Brook University, New York, USA, 12-16 April 2021  
doi:10.21468/SciPostPhysProc.?*

## Abstract

This analysis extends recent measurements of the jet sub-structure observables based on the SoftDrop algorithm in  $p+p$  collisions at  $\sqrt{s} = 200$  GeV in the STAR experiment. We present fully unfolded multi-differential measurements of jet sub-structure observables at the first split and their correlations for jets of different transverse momenta and radii. We compare our measurements to various Monte Carlo models.

## 1 Introduction

Jets are collimated sprays of hadrons that are produced in high energy particle collisions. Jet sub-structure measurements serve as an experimental tool for studying Quantum Chromodynamics (QCD) and parton shower evolution. Evolution of hard scattered partons is described via a shower algorithm based on both momentum and angular scales. In order to better assess the jet sub-structure, it is necessary to use a jet grooming technique such as SoftDrop [1]. This technique connects parton shower and angular tree, and removes soft radiations within a jet. In the SoftDrop framework, when a jet is reconstructed using the anti- $k_T$  algorithm [2], it is reclustered with the C/A algorithm [3] to get an angular ordered tree. The jet is then divided into two sub-jets, labeled as 1 and 2, by undoing the last step of the C/A algorithm. If the two sub-jets pass the SoftDrop condition

$$\frac{\min(p_{T,1}, p_{T,2})}{p_{T,1} + p_{T,2}} > z_{\text{cut}} \left( \frac{\Delta R_{1,2}}{R} \right)^\beta, \quad (1)$$

then the jet is considered as the final SoftDrop jet. In Eq. 1,  $p_{T,i}$  corresponds to the transverse momentum of the sub-jet,  $\Delta R_{1,2}$  is the distance between sub-jets and  $R$  is the resolution parameter. If the condition is not met, the sub-jet with the higher  $p_T$  is denoted as the starting jet and the whole process is repeated until the condition is met. The SoftDrop procedure depends on two parameters,  $\beta$  and  $z_{\text{cut}}$ , which are set to  $\beta = 0$  and  $z_{\text{cut}} = 0.1$ . The products of this procedure are two jet sub-structure observables, shared momentum fraction ( $z_g$ ) and groomed radius ( $R_g$ ). The shared momentum fraction is defined as  $z_g = \frac{\min(p_{T,1}, p_{T,2})}{p_{T,1} + p_{T,2}}$  and the groomed radius is defined as the first  $\Delta R_{1,2}$  that satisfies the SoftDrop condition.

In the previous STAR measurements [4], the momentum and angular scales were measured independently via SoftDrop observables,  $z_g$  and  $R_g$ , for jets of varying transverse momenta and

35 resolution parameters. Our goal is to extend previous measurements and study the correlation  
 36 between the observables  $z_g$  and  $R_g$  as a function of jet transverse momentum ( $p_{T,\text{jet}}$ ). Another  
 37 way to explore the jet sub-structure is to use the Lund Plane diagram [5]. This theoretical  
 38 toolkit represents the phase-space of the jet evolution by a 2D triangular plane of the transverse  
 39 momenta and the angles of emissions with respect to their emitters. Recent ATLAS and ALICE  
 40 measurements of the Lund Plane [6,7] showed significant differences in the groomed jet radius  
 41 between models with varying hadronization and parton shower implementations. We explore  
 42 these differences via SoftDrop observables at lower  $p_T$  than LHC measurements, where non-  
 43 perturbative effects are expected to be larger.

## 44 2 Data analysis

45 Data for this analysis were collected by the STAR experiment [8] in 2012 for  $p+p$  collisions at  
 46  $\sqrt{s} = 200$  GeV. Events are triggered via a  $1 \times 1$  patch in pseudorapidity  $\times$  azimuthal angle ( $\eta \times \phi$ )  
 47 in the Barrel Electromagnetic Calorimeter (BEMC) [9] with a total transverse energy  $E_T > 7.3$   
 48 GeV. Jets are reconstructed using charged-particle tracks from the Time Projection Chamber  
 49 (TPC) [10] and BEMC towers in the range  $0.2 < p_T(E_T) < 30$  GeV/c (GeV). Reconstructed  
 50 charged-particle tracks are matched to BEMC towers and hadronic correction is applied to  
 51 avoid double counting of charged-particle tracks' energies deposited in the BEMC.

52 Jets are reconstructed with the anti- $k_T$  algorithm for two values of resolution parameter,  $R$   
 53  $= 0.4$  and  $R = 0.6$ . They are required to have  $p_{T,\text{jet}} > 10$  GeV/c and to lie within the pseudo-  
 54 rapidity  $|\eta_{\text{jet}}| < 1.0 - R$  to assure that the jet cone is fully contained in the STAR acceptance.

55 Since the measurement is affected by finite efficiency and detector resolution, these ef-  
 56 fects have to be deconvolved to obtain particle-level distributions. These observables lie in  
 57 3-dimensional space,  $(p_{T,\text{jet}}, z_g, R_g)$ , and thus multi-dimensional unfolding is needed. The 2D  
 58 unfolding for  $(z_g, R_g)$  is done with a response matrix which contains particle-level and detector-  
 59 level distributions. Particle-level distributions are obtained from the PYTHIA 6 events [11]  
 60 with the STAR Perugia tune [12]. They are then passed through the GEANT3 detector sim-  
 61 ulation [13] and embedded into zero-bias events to obtain detector-level distributions. We  
 62 apply an iterative Bayesian unfolding [14], implemented in the RooUnfold framework [15],  
 63 on measured 2D  $(z_g, R_g)$  distributions in four different detector-level  $p_{T,\text{jet}}$  intervals, namely,  
 64  $p_{T,\text{jet}}^{\text{det}} \in [15,20], [20,25], [25,30],$  and  $[30,40]$  GeV/c. Following the removal of the detector  
 65 effects on the sub-structure observables, the correction for  $p_{T,\text{jet}}$ , due to jet energy scale and  
 66 resolution effects, is applied as follows. Projections of the detector level jet  $p_T$  distributions are  
 67 obtained from the jet  $p_T$  response matrix (Fig. 1 in [4]) for selected particle-level  $p_T$  intervals  
 68 used in this measurement. These projections are then normalized to unity and used as weights  
 69 to be applied to unfolded  $z_g$  vs.  $R_g$  distributions, followed by a correction for the jet finding  
 70 efficiency, resulting in 3D fully corrected measurements in selected particle-level  $p_T$  intervals.

71 Systematic uncertainties on our measurements are estimated from the following sources -  
 72 tracking efficiency, tower energy scale, hadronic correction and unfolding. These are the same  
 73 sources which are explored in previous jet sub-structure measurement [4]. The first source of  
 74 the systematic uncertainty is the hadronic correction, which is evaluated by varying the fraction  
 75 of track momentum subtracted from the nominal value of 100% to 50%. The precision of the  
 76 BEMC tower calibration is 3.8% and the uncertainty in the TPC tracking efficiency is 4%. The  
 77 systematic uncertainty coming from the unfolding method is estimated by varying the iteration  
 78 parameter from 4 to 6. The systematic uncertainty due to the prior shape variation has not  
 79 been estimated yet and will be included in the forthcoming publication. An example of the  
 80 magnitudes of each individual systematic uncertainty and total systematic uncertainty for  $z_g$   
 81 distributions in three  $R_g$  intervals for jets with  $R = 0.4$  and  $20 < p_{T,\text{jet}} < 25$  GeV/c is plotted in

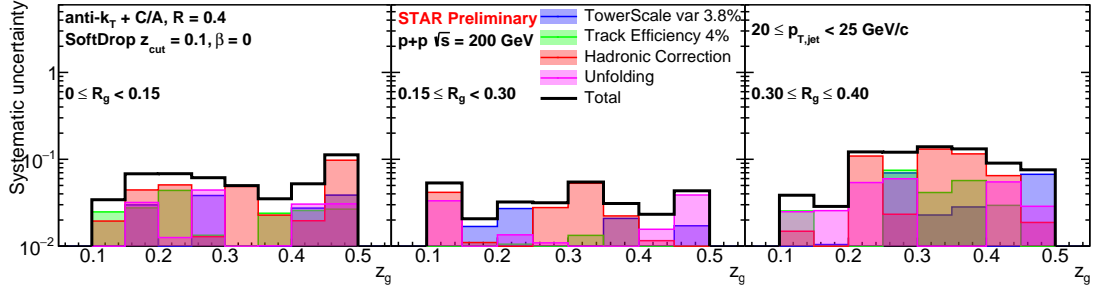


Figure 1: Systematic uncertainties for  $z_g$  in three  $R_g$  bins for jets with  $R = 0.4$  and  $20 < p_{T,jet} < 25 \text{ GeV}/c$ .

82 Fig. 1. The largest contribution comes from the hadronic correction and unfolding. The total  
83 uncertainty is typically about 5-10%.

### 84 3 Results and Monte Carlo comparisons

85 Fully unfolded  $z_g$  vs.  $R_g$  distributions for four different  $p_{T,jet}$  intervals and  $R = 0.4$  are shown in  
86 Fig. 2. Bands around the data points correspond to the total systematic uncertainties discussed  
87 in Sec. 2. We observe a significant change to the shape of the  $z_g$  distributions as the  $R_g$  is varied.  
88 Jets with a large  $R_g$  tend to have steeper  $z_g$  distributions representing an enhanced probability  
89 of softer splits as compared to jets with a smaller  $R_g$  which consequently have a much flatter  $z_g$   
90 due to collinear hard splittings. The dependence on the  $p_{T,jet}$  is observed to be small compared  
91 to the  $R_g$  which essentially determines the shape of the  $z_g$ .

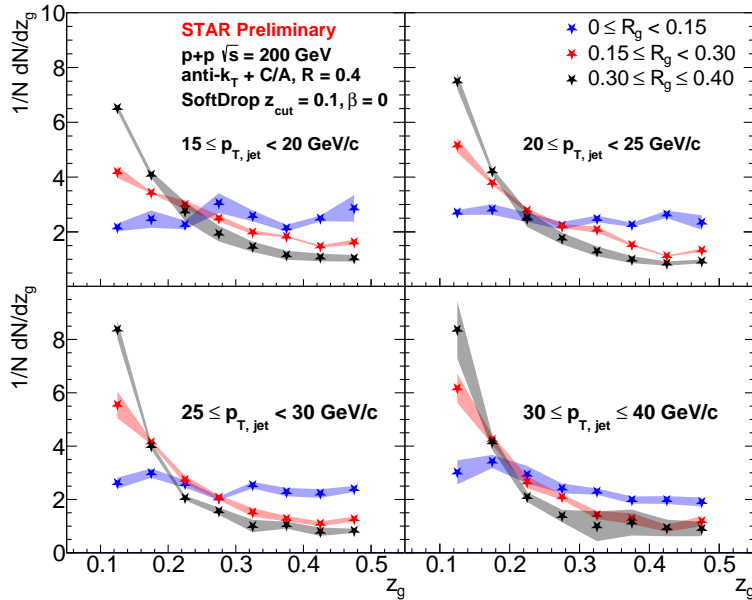


Figure 2: Fully unfolded  $z_g$  distributions for three  $R_g$  bins for jets with  $R = 0.4$  in  $p+p$  collisions at  $\sqrt{s} = 200 \text{ GeV}$ . Individual panels correspond to different  $p_{T,jet}$  intervals (see legend).

92 In Fig. 3, a comparison of the unfolded  $z_g$  vs.  $R_g$  distributions for different resolution

93 parameters,  $R = 0.4$  on the left and  $R = 0.6$  on the right, is shown. In this case, the distributions  
 94 are shown only for two  $R_g$  bins,  $0 < R_g < 0.15$  and  $0.15 < R_g < 0.30$ . In both cases, the  
 95 distributions look very similar, which shows that the choice of jet radius does not significantly  
 96 affect the jet sub-structure.

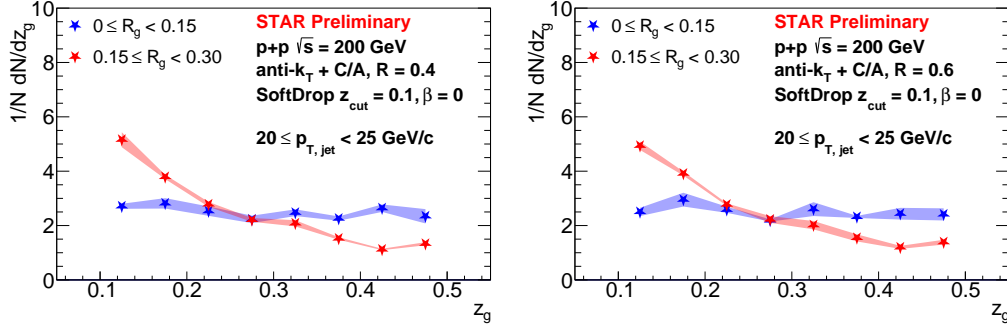


Figure 3: Fully unfolded  $z_g$  distributions in two  $R_g$  bins for jets with  $20 < p_{T,\text{jet}} < 25$  GeV/c and  $R = 0.4$  (left) or  $R = 0.6$  (right).

97 The fully corrected  $z_g$  distributions are compared with several Monte Carlo (MC) models,  
 98 such as PYTHIA 6 with Perugia 2012 tune, PYTHIA 8 [16] with the Monash tune based on  
 99 LHC data [17] and HERWIG 7 [18] with the EE5C underlying event tune [19]. There are  
 100 differences in parton shower implementations in these MC generators. In HERWIG, the parton  
 101 shower is angularly ordered whereas both PYTHIA versions employ  $k_T/p_T$  ordering. There are  
 102 also differences in the hadronization models, i. e. PYTHIA uses the Lund string model whereas  
 103 HERWIG is based on the cluster model.

104 The comparison of  $z_g$  distributions in three different  $R_g$  bins for jets with  $R = 0.4$  and  $20$   
 105  $< p_{T,\text{jet}} < 25$  GeV/c between data and MC simulations is displayed in Fig. 4. All of the MC  
 106 models describe the trend observed in data. There are slight differences between the models  
 107 especially for the most narrow splittings which will be followed up to disentangle the impact  
 108 of perturbative and non-perturbative QCD effects.

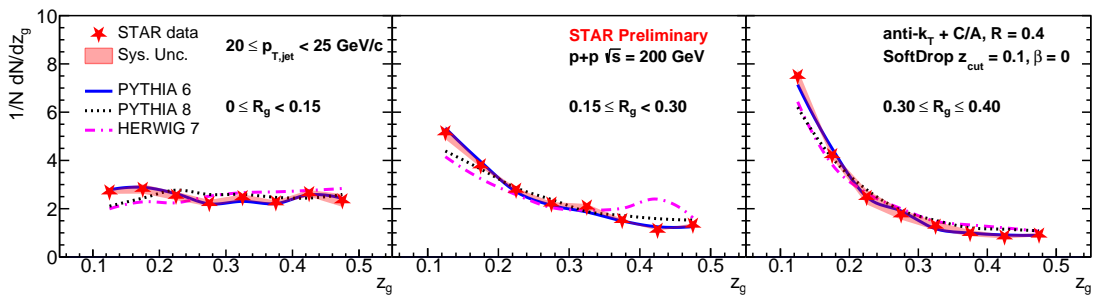


Figure 4: Fully unfolded  $z_g$  distributions in three  $R_g$  bins for jets with  $R = 0.4$  and  $20 < p_{T,\text{jet}} < 25$  GeV/c in  $p+p$  collisions at  $\sqrt{s} = 200$  GeV, compared with Monte Carlo simulations.

## 109 4 Conclusion

110 We presented the first measurement of correlations between jet sub-structure observables  $z_g$   
 111 vs.  $R_g$  in different  $p_{T,\text{jet}}$  intervals utilizing the 2+1D unfolding method.  $z_g$  distributions show a

112 strong dependence on  $R_g$  and weak dependence on  $p_{T,\text{jet}}$ , which allows us to isolate soft splits  
113 by selecting wide angle splits. The distributions are compared with Monte Carlo simulations,  
114 all of which capture the trend observed in data. The next steps of our analysis will focus  
115 on disentangling perturbative and non-perturbative QCD effects in the MC simulations and  
116 extending to comparisons with theoretical calculations.

## 117 References

- 118 [1] A. J. Larkoski, S. Marzani, G. Soyez and J. Thaler, *Soft Drop*, Journal of High Energy  
119 Physics **2014**(5) (2014), doi:[10.1007/JHEP05\(2014\)146](https://doi.org/10.1007/JHEP05(2014)146).
- 120 [2] M. Cacciari, G. P. Salam and G. Soyez, *The anti- $k_t$  jet clustering algorithm*, Journal of  
121 High Energy Physics **2008**(04), 063 (2008), doi:[10.1088/1126-6708/2008/04/063](https://doi.org/10.1088/1126-6708/2008/04/063).
- 122 [3] *A Cambridge-Aachen (C-A) based Jet Algorithm for boosted top-jet tagging* (2009).
- 123 [4] J. Adam et al., *Measurement of Groomed Jet Substructure Observables in  $p+p$  Col-*  
124 *lisions at  $\sqrt{s_{NN}} = 200$  GeV with STAR*, Physics Letters B **811**, 135846 (2020),  
125 doi:<https://doi.org/10.1016/j.physletb.2020.135846>.
- 126 [5] F. A. Dreyer, G. P. Salam and G. Soyez, *The Lund jet plane*, Journal of High Energy Physics  
127 **2018**(12) (2018), doi:[10.1007/JHEP12\(2018\)064](https://doi.org/10.1007/JHEP12(2018)064).
- 128 [6] G. Aad et al., *Measurement of the Lund Jet Plane Using Charged Particles in 13 TeV Proton-*  
129 *Proton Collisions with the ATLAS Detector*, Physical Review Letters **124**(22), 222002  
130 (2020), doi:[10.1103/PhysRevLett.124.222002](https://doi.org/10.1103/PhysRevLett.124.222002).
- 131 [7] L. Havener, *Jet splitting measurements in Pb–Pb and pp collisions at  $\sqrt{s_{NN}} = 5.02$  TeV with*  
132 *ALICE*, Nuclear Physics A **1005** (2021), doi:[10.1016/j.nuclphysa.2020.121906](https://doi.org/10.1016/j.nuclphysa.2020.121906).
- 133 [8] K.H. Ackermann et al., *Star detector overview*, Nuclear Instruments and Methods  
134 in Physics Research Section A: Accelerators, Spectrometers, Detectors and Associated  
135 Equipment **499**(2), 624 (2003), doi:[https://doi.org/10.1016/S0168-9002\(02\)01960-](https://doi.org/10.1016/S0168-9002(02)01960-5)  
136 [5](https://doi.org/10.1016/S0168-9002(02)01960-5).
- 137 [9] T. M. Cormier et al., *STAR barrel electromagnetic calorimeter absolute calibration using*  
138 *“minimum ionizing particles” from collisions at RHIC*, Nuclear Instruments and Methods  
139 in Physics Research Section A: Accelerators, Spectrometers, Detectors and Associated  
140 Equipment **483**(3), 734 (2002), doi:[10.1016/S0168-9002\(01\)01951-9](https://doi.org/10.1016/S0168-9002(01)01951-9).
- 141 [10] M. Anderson et al., *The STAR time projection chamber*, Nuclear Instruments and Methods  
142 in Physics Research Section A: Accelerators, Spectrometers, Detectors and Associated  
143 Equipment **499**(2-3), 659 (2003), doi:[10.1016/S0168-9002\(02\)01964-2](https://doi.org/10.1016/S0168-9002(02)01964-2).
- 144 [11] T. Sjöstrand, S. Mrenna and P. Skands, *PYTHIA 6.4 physics and manual*, Journal of High  
145 Energy Physics **2006**(05), 026 (2006-05-01), doi:[10.1088/1126-6708/2006/05/026](https://doi.org/10.1088/1126-6708/2006/05/026).
- 146 [12] P. Z. Skands, *Tuning Monte Carlo generators*, Physical Review D **82**(7) (2010),  
147 doi:[10.1103/PhysRevD.82.074018](https://doi.org/10.1103/PhysRevD.82.074018).
- 148 [13] R. Brun, R. Hagelberg, M. Hansroul and J. C. Lassalle, *Geant: Simulation Program for*  
149 *Particle Physics Experiments. User Guide and Reference Manual* (1978).

- 150 [14] G. D'Agostini, *A multidimensional unfolding method based on bayes' theorem*, Nu-  
151 clear Instruments and Methods in Physics Research Section A: Accelerators, Spectrom-  
152 eters, Detectors and Associated Equipment **362**(2-3), 487 (1995), doi:[10.1016/0168-  
153 9002\(95\)00274-X](https://doi.org/10.1016/0168-9002(95)00274-X).
- 154 [15] T. Auye, *Unfolding algorithms and tests using RooUnfold*, In *PHYSTAT 2011*. CERN,  
155 Geneva, doi:[10.5170/CERN-2011-006.313](https://doi.org/10.5170/CERN-2011-006.313) (2011), [1105.1160](https://arxiv.org/abs/1105.1160).
- 156 [16] T. S. et al., *An introduction to PYTHIA 8.2*, Computer Physics Communications **191**, 159  
157 (2015), doi:[10.1016/j.cpc.2015.01.024](https://doi.org/10.1016/j.cpc.2015.01.024).
- 158 [17] P. Skands, S. Carrazza and J. Rojo, *Tuning PYTHIA 8.1*, The European Physical Journal  
159 C **74**(8) (2014), doi:[10.1140/epjc/s10052-014-3024-y](https://doi.org/10.1140/epjc/s10052-014-3024-y).
- 160 [18] J. Bellm et al., *Herwig 7.0/Herwig++ 3.0 release note*, The European Physical Journal C  
161 **76**(4) (2016), doi:[10.1140/epjc/s10052-016-4018-8](https://doi.org/10.1140/epjc/s10052-016-4018-8).
- 162 [19] M. Seymour and A. Siodmok, *Constraining MPI models using eff and recent Teva-*  
163 *tron and LHC Underlying Event data*, Journal of High Energy Physics **2013** (2013),  
164 doi:[10.1007/JHEP10\(2013\)113](https://doi.org/10.1007/JHEP10(2013)113).